Wood Sci Technol (2018) 52:445–463
https://doi.org/10.1007/s00226-018-0986-1

ORIGINAL

Regional calibration models for predicting loblolly pine tracheid properties using near-infrared spectroscopy

Mohamad Nabavi[1] · Joseph Dahlen[1] · Laurence Schimleck[2] · Thomas L. Eberhardt[3] · Cristian Montes[1]

Received: 23 June 2017 / Published online: 16 January 2018

Abstract This study developed regional calibration models for the prediction of loblolly pine (*Pinus taeda*) tracheid properties using near-infrared (NIR) spectroscopy. A total of 1842 pith-to-bark radial strips, aged 19–31 years, were acquired from 268 trees from 109 stands across the southeastern USA. Diffuse reflectance NIR spectra were collected at 10-mm increments from the radial face of pith-to-bark strips using a FOSS 5000 scanning spectrometer. A subset of the 10-mm samples was selected based on the NIR spectra uniqueness and placed in calibration ($N = 1020$) and validation ($N = 998$) test sets. The samples were macerated and the tracheid properties measured using an optical analyzer (Techpap MorFi Fiber and Shive Analyzer). Models were created using partial least squares (PLS) regression using the calibration samples, and their performance checked using the validation set. Prediction PLS models for tracheid length were strong when checked with the validation set [$R_p^2 = 0.87$, standard error of prediction (SEP) = 0.23 mm, ratio of performance to deviation (RPD) = 2.8]. Prediction models for tracheid width had moderate fit statistics ($R^2 = 0.61$, SEP = 1.6 μm, RPD = 1.6), but the SEP was similar to the measurement error of the camera (± 2 μm). The NIR wavelengths of importance were largely attributed to cellulose. The 1542 nm wavelength explained 77% of the variation in tracheid length (RMSE = 0.31 mm). These results demonstrate that NIR spectroscopy models for tracheid length and width can be developed from a diverse set of samples and still maintain prediction accuracy.

✉ Joseph Dahlen
jdahlen@uga.edu

1 Warnell School of Forestry and Natural Resource, University of Georgia, 180 E Green Street, Athens, GA 30602-2152, USA

2 Wood Science and Engineering, Oregon State University, 119 Richardson Hall, Corvallis, OR 97331, USA

3 USDA Forest Products Laboratory, One Gifford Pinchot Drive, Madison, WI 53726, USA

Introduction

The southeastern region of the USA produces approximately half of the total wood produced in the USA, and approximately 16% of wood consumed worldwide (Wear and Greis 2002; Zhao et al. 2011). Over 13 million hectares of southern pine, composed of loblolly pine (*Pinus taeda*), slash pine (*Pinus elliottii*), longleaf pine (*Pinus palustris*), and shortleaf pine (*Pinus echinata*), have been established (Wear and Greis 2002). Of the southern pines, loblolly pine is the most commercially important species owing to its ability to survive on a broad range of sites and fast growth (Schultz 1997; McKeand et al. 2003; Zhao et al. 2011). It has been extensively improved for growth and stem quality through genetic selection (McKeand et al. 2003), and research trials have demonstrated growth rates of 29.4 m^3/ha per year (Borders and Bailey 2001). These fast growth rates have led to rotation ages being decreased to 25 years or less (Fox et al. 2007), achieving site indexes as high as 32 m (base age 25) (Zhao et al. 2016). As rotation ages decrease, there is significant concern regarding the quality of wood produced due to a greater proportion of corewood (aka juvenile wood) and how its properties can impact the overall performance of wood and fiber-based products (White et al. 2009; Moore and Cown 2017). The presence of corewood is particularly prevalent in pulpwood, typically harvested during thinning operations and from treetops at final harvest.

Regarding pulp and paper properties, these are strongly influenced by tracheid morphological properties including length, width, and cell wall thickness (Zobel and Van Buijtenen 1989; McKenzie 1994; Via et al. 2004; Pulkkinen et al. 2006; Smook 2016). Tracheid length affects the tensile strength of paper, and it is critical for maintaining wet web strength (Niskanen 1998). Tracheid width and cell wall thickness have a strong influence on fibers ability to collapse during papermaking (Paavilainen 1993). Tracheids with larger diameters and thin cell walls produce paper with improved strength and smoothness (Wang and Aitken 2001).

Traditional methods used to measure tracheid properties rely on time-consuming sample macerations, typically following the technique described by Franklin (1945) where wood is macerated under elevated temperatures in a solution of acetic acid, hydrogen peroxide, and water. Tracheid length is then measured via microscope or optical image analyzer (Hirn and Bauer 2006). With a microscope only non-cut tracheids are measured so mean length and width are typically reported. An optical analyzer does not differentiate between non-cut and cut tracheids, and thus, the traditional length metric reported is weighted length which is roughly comparable to the mean tracheid length as measured on a microscope (Chen et al. 2016a). To analyze large numbers of samples generated from field studies, rapid and cost-effective methods are needed (Schimleck et al. 2003). With the SilviScan system, an automated cell wall scanner measures the radial and tangential diameters of tracheids, with wall thickness and coarseness then calculated from the tracheid diameters and density measurements collected from an X-ray densitometry (Evans 1994). As an alternative to the SilviScan system, Vahey et al. (2007) developed a high-resolution wood cell scanner prototype to measure density and tracheid dimensions using only image analysis. Direct measurement of tracheid length has occasionally been done on solid samples (Ladell 1959; Wilkins and Bamber 1983); however, few studies have utilized this technique since the introduction of automated fiber analyzers that work on macerated samples.

Near-infrared (NIR) spectroscopy has also been used to provide rapid estimations of a variety of wood properties (So et al. 2004; Mora and Schimleck 2008; Tsuchikawa and Schwanninger 2013; Tsuchikawa and Kobori 2015). Significant work has been conducted on measuring wood chemistry-related information (Raymond and Schimleck 2002; Hodge and Woodbridge 2004; Yeh et al. 2004; Jones et al. 2006; Tsuchikawa 2007), pulp yield (Schimleck and French 2002; Schimleck et al. 2006), specific gravity (Schimleck et al. 2003), microfibril angle (MFA) (Schimleck et al. 2003; Jones et al. 2005b), and mechanical properties (Gindl et al. 2001; Kelley et al. 2004; Schimleck et al. 2005; Haartveit and Flæte 2006; Hein et al. 2010).

The use of NIR spectroscopy could be particularly attractive for predicting tracheid length because the common measurement techniques require macerated samples, but compared to other wood anatomical properties, it has attracted little attention. Schimleck et al. (2004a) analyzed radial strips collected at breast height from 14 loblolly pine trees from four sites and found strong relationships between measured and NIR-predicted tracheid lengths (coefficient of determination for prediction set (R_p^2) = 0.88, standard error prediction (SEP) = 0.25 mm) and a ratio of performance to deviation (RPD) of 2.5. Via et al. (2005b) analyzed approximately 60 disks collected at various heights from 10 longleaf pine trees from a single site and found a good relationship between measured and NIR-predicted tracheid lengths ($R_p^2 = 0.65$, SEP not reported). Inagaki et al. (2012) examined the feasibility of using NIR spectroscopy for nondestructive evaluation of fiber length measured using a microscope in 50 samples of *Eucalyptus camaldulensis* from a single tree and obtained strong predictions ($R_p^2 = 0.98$, SEP = 0.012 mm) and a RPD of 2.8. Pereira et al. (2015), using an optical fiber analyzer, reported strong predictions for fiber length ($R_p^2 = 0.94$, SEP = 0.007 mm, RPD = 3.9) and fiber width ($R_p^2 = 0.90$, SEP = 0.36 µm, RPD = 3.3) for *Acacia melanoxylon* collected from 20 trees collected from four sites in Portugal; the samples were obtained from kraft pulp, differing from most studies which macerate wood fibers using the Franklin (1945) technique. Altogether, the good model statistics acquired in these studies suggests that NIR spectroscopy is a suitable tool for rapid prediction of tracheid and fiber length.

Lacking in the literature are calibration models for tracheid properties developed from a broader range of sites that capture the regional variation (Jordan et al. 2008) that exists in a given species; capturing this information is critical if NIR is to be used more broadly. To explore the feasibility of NIR models incorporating a range of sites and species, Hodge and Woodbridge (2004) developed calibration models for lignin content from 174 breast height cores from five pine species growing in Brazil and Colombia and found strong relationships between measured and NIR-predicted lignin contents ($R_p^2 = 0.91$, SEP = 0.4%), indicating that broad-based models for wood chemistry are feasible. Schimleck et al. (2010) developed calibrations for density, microfibril angle (MFA), and modulus of elasticity (MOE) from 370 breast height cores from 14 pine species samples collected from Argentina, Brazil, Chile, Colombia, and South Africa. The combined species data yielded good relationships for density (R_p^2 = 0.71, SEP = 47 kg/m^3, RPD = 1.8), MFA (R_p^2 = 0.79, SEP = 4.7°, RPD = 2.1), and MOE (R_p^2 = 0.86, SEP = 1.5 GPa, RPD = 2.7); these results suggest that NIR spectroscopy can be used to develop calibration models for wood anatomical, physical, and mechanical properties. Here, the goals of this study were to: (1) develop regional calibration models for the prediction of tracheid properties (length and width) using NIR from loblolly pine samples collected from across the southeastern USA, and (2) explore the relationship between measured tracheid properties and NIR wavelengths associated with cellulose, hemicellulose, and lignin.

Materials and methods

Specimen origin

The loblolly pine samples used here are from the Wood Quality Consortium baseline study (Jordan et al. 2008; Antony et al. 2010); 134 stands were sampled from six physiographic regions: (1) Southern Atlantic Coastal Plain, (2) Northern Atlantic Coastal Plain, (3) Upper Coastal Plain, (4) Piedmont, (5) Gulf Coastal Plain, and (6) Hilly Coastal region. The stands did not have intensive silviculture applied (i.e., fertilization or competition control) with the exception of phosphorus-deficient sites that were fertilized at stand establishment. From each stand, three trees were felled and 2.5-cm-thick wood disks were cut at 1.5-m intervals from the base to a top diameter of 2.5 cm except for the disk at breast height which was extracted at 1.37 m. Each disk usually yielded two sets of two book-matched pith-to-bark radial strips cut 12 mm high by 12 mm wide which were then dried to approximately 12% moisture content. For this study, some of the baseline study radial strips were not available, having been used in prior studies involving determinations of ring-by-ring specific gravity (Antony et al. 2010), microfibril angle (Jordan et al. 2007), the feasibility of using NIR spectroscopy for measuring tracheid length (Schimleck et al. 2004a), tracheid morphology obtained from SilviScan (Schimleck et al. 2004b; Jones et al. 2005a), and wood chemistry (Jones et al. 2006). Unfortunately, some radial strips were found to have blue stain and were therefore excluded because blue stain has been shown to cause erroneous relationships with NIR spectroscopy (Via et al. 2005a). Altogether, a total of 1842 radial strips from 268 trees and 109 stands were available for this study (Fig. 1). Table 1 shows the breakdown of radial strips and a summary of the tree information for this study.

Near-infrared spectroscopy

A FOSS NIRSystems Model 5000 scanning grating spectrophotometer (FOSS NIRSystems, Inc., Laurel, MD) with a diffuse reflectance static module was used to scan the wood strips on the radial face. The spectra were collected at 2-nm interval over the wavelength range 1100–2500 nm. The instrument reference was a ceramic

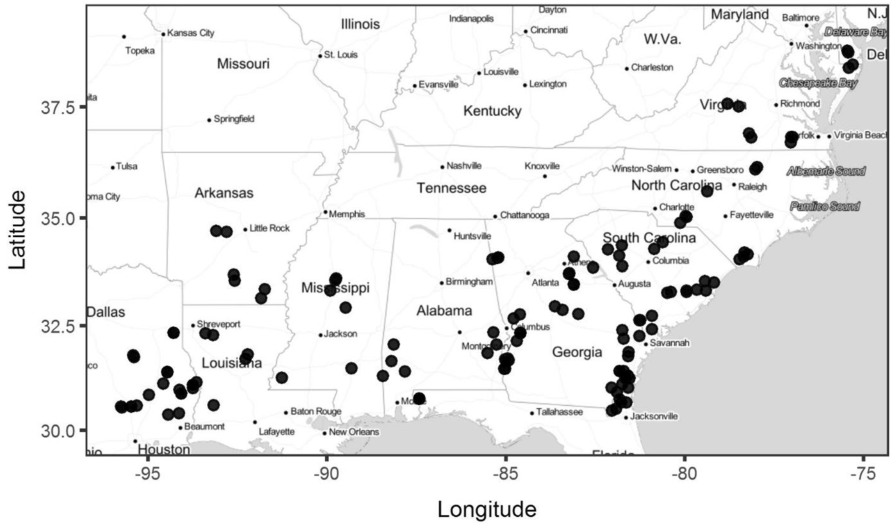

Fig. 1 Location of the 109 loblolly pine stands sampled from across the southeastern USA

Table 1 Stand characteristics and locations

Region	*N*					Age		DBH (cm)		Height (m)	
	Stands	Trees	Disks	10-mm sections	Macerated	Mean	SD	Mean	SD	Mean	SD
1	32	76	403	2503	487	22	1.6	23.8	4.7	20.6	2.5
2	7	17	105	710	164	22	1.9	24.3	3.7	18.1	2.7
3	12	29	233	1508	266	23	1.5	23.1	4.5	19.2	3.1
4	16	27	129	750	162	23	1.9	23.2	4.3	18.0	1.8
5	16	45	342	1943	317	23	3.6	20.4	3.8	18.9	2.7
6	26	74	630	4014	622	23	3.2	23.2	4.3	19.5	2.9
Overall	109	268	1842	11,428	2018	23	2.4	23.0	4.5	19.4	2.8

Region: 1 = Lower Coastal Plain, 2 = North Atlantic, 3 = Upper Coastal Plain, 4 = Piedmont, 5 = Gulf Coastal Plain, 6 = Hilly Coastal

standard provided by the manufacturer. Radial strips were conditioned for at least 4 weeks in a 20 °C and 40% relative humidity-controlled environment room (~ 7.7% moisture content). To concentrate the light on a constant area of the sample, a Teflon mask with a window measuring 5 mm high × 10 mm wide was applied to allow for 10-mm NIR scans from pith to bark. Fifty scans were completed and averaged to attain a single spectrum for each 10-mm section. Each radial strip was marked into 10-mm sections from pith to bark on the transverse face prior to NIR scanning. Following each 10-mm scan, the radial strips were moved 10-mm radially using a custom-made auto-sampler consisting of a Parker servo motor and controller, and a linear stage; this system allowed for the pith-to-bark scans at 10-mm intervals (Jones et al. 2007). The NIR scanning was done in the controlled environment room.

The 1842 radial strips produced 11,428 NIR spectra. The NIR spectra pretreatment used was a second derivative with left and right gaps of 4 nm using the Savitzky–Golay approach (Savitzky and Golay 1964). Because it was not feasible to macerate all 10-mm sections, principal component analysis (PCA) and the Duplex sample selection technique (modified Kennard-Stone) (Kennard and Stone 1969; Snee 1977) were used to split the 10-mm samples into calibration and validation sets. The Duplex algorithm selects the most unique samples based on the Mahalanobis distance, which helps ensure that the calibration and validation sets contained samples representative of the population while still maintaining independence between the calibration and validation sets (Snee 1977; Mora and Schimleck 2008). To further maintain independence with the data, when a 10-mm section was selected from a radial strip for the calibration set, other 10-mm sections from the same radial strip were not included in the validation set, and vice versa. The 11,428 10-mm sections were split into calibration ($N = 547$), validation ($N = 547$), and the prediction sets ($N = 10{,}334$). Following the sample selection procedure, all of the samples collected from the breast height disks (1.37 m) were also included for maceration. These samples were removed from the prediction set and placed into the calibration or validation set as determined by the sample selection algorithm. Thus, the study consisted of a calibration ($N = 1020$), validation ($N = 998$) and prediction ($N = 9410$) set. No samples from the final prediction set were macerated and analyzed for tracheid properties.

Tracheid properties

Following the sample selection procedure, the selected sections for the calibration and validation sets were cut from the radial strips into individual 10-mm sections using a razor blade. The sections were further cut into 2-mm sections using a razor blade. The samples were then macerated with 30 mL of 50% hydrogen peroxide, 20 mL of water, and 50 mL glacial acetic acid at 60 °C for 48 h (Franklin 1945). The maceration schedule was selected after several trials with different times and temperatures; the final schedule worked well at separating but not deteriorating the tracheids. After 48 h, the tracheids and chemicals were cooled to room temperature; then, the tracheids were separated from the pulping chemicals using a Buchner funnel, rinsed with approximately 1.9 L of water, and then, the acidic spent chemicals and the rinse water were neutralized with sodium carbonate. The rinsed tracheids were gently shaken in water for a few seconds to further separate them from each other and then diluted with approximately 1 L of water prior to analysis. It was observed that the tracheids would begin to break down if left in the room-temperature maceration solution for more than 2 days following the maceration process; thus, the samples were all neutralized within 2 days. The macerated samples were analyzed using a TechPap MorFi Compact Fiber and Shive Analyzer with a 4-μm resolution camera (Techpap SAS, France) to assess tracheid properties. The equipment measured the number of tracheids, frequency of tracheids, tracheid length, and width using image analysis. To further separate the tracheids from each other, it was found that running the tracheids through the MorFi for approximately 2 min prior to image analysis would result in complete separation of the tracheids from each other. For each sample, approximately 2500 tracheids were analyzed. The length-weighted tracheid length and the width-weighted tracheid width were used for the calculations instead of the mean value to minimize the effect of fines and cut tracheids (Carvalho et al. 1997). Length-weighted tracheid length is calculated by:

$$L_1 = \frac{\Sigma_{n_i l_i^2}}{\Sigma_{n_i l_i}} \tag{1}$$

where L_1 is length-weighted tracheid length, n_i is number of tracheids in the ith class, and l_i is the mean length of the ith class (Carvalho et al. 1997), and width-weighted tracheid width was calculated similarly.

Calibration and prediction of tracheid properties

All statistical analysis was conducted using R (R Core Team 2017) with RStudio interface (RStudio 2017) and the following packages: chemometrics (Varmuza and Filzmoser 2009), dplyr (Wickham and Francois 2016), ggmap (Kahle and Wickham 2013), ggplot2 (Wickham 2009), pls (Mevik et al. 2013), prospectr (Stevens and Ramirez-Lopez 2013), and signal (Signal developers 2013). Calibration models were developed on the original and the smoothed second-derivative data using PLS regression with four cross-validation segments and a maximum of 10 factors considered. The final number of factors was determined based on the standard error of cross-validation (SECV) (determined from the residuals of the final cross-validation), the root-mean-square error of cross-validation (RMSECV), the coefficient of determination of cross-validation (R^2), and the RPD for the cross-validation (RPDcv) (Williams and Sobering 1993). The RPDcv was calculated as the ratio of the standard deviation of the reference data to the SECV. Determination of RPDcv allows comparison of calibrations developed for different wood properties that have differing data ranges and units, the higher the RPDcv, the more accurate the data are described by the calibration (Granato and Ares 2013).

The performance of the calibration models was examined by predicting the wood properties of the validation set samples. The standard error of prediction (SEP) (determined from the residuals of the predictions for the validation set) was calculated and gives a measure of how well a calibration model predicts parameters of interest for a separate set of samples (i.e., samples not included in the calibration set). The predictive ability of the calibration models was assessed by the coefficient of determination (R_p^2) and calculating the RPDp, which is similar to the RPDcv but uses the standard deviation of the validation set reference data, and the SEP.

Jones et al. (2005a) demonstrated that the prediction accuracy of tracheid property predictions for new sites can be improved considerably when the addition of one sample from the new site is added to the calibration model. A calibration model, if built from a large enough sample size, may be able to be applied to new sites without the addition of new samples added to the model. To determine whether this was effective, separate calibration models for tracheid length and width were constructed from samples collected from an individual region and then applied to samples from the other regions. Thus, the prediction accuracy was determined when NIR calibration models, built from large datasets, are applied to new datasets.

In order to attribute NIR wavelengths of importance to those wavelengths associated with wood chemistry information, NIR bands were assigned via a quantitative approach. For each wavelength (1100–2500 nm), linear regression models were conducted to relate tracheid length with each band. The linear regression model coefficient of determination (R^2) was plotted for each wavelength and the peaks (local maxima) found through the derivatives. The local maxima peaks with $R^2 > 0.35$ were considered initially as bands of importance and then compared to the assignments compiled by Schwanninger et al. (2011). The bands that were local maxima but those not assigned to cellulose, hemicellulose, or lignin by Schwanninger et al. (2011) were removed from consideration because the intent was to find those wavelengths attributed to wood chemistry as found in the literature. Multiple linear regressions models using stepwise regression were constructed between tracheid properties and the identified bands of importance.

Results and discussion

Tracheid properties for the calibration and validation datasets are presented in Table 2; these summary statistics are based on measurements of approximately 5.1 million tracheids. A total of 1020 NIR spectra were used to develop the calibration model, and 998 NIR spectra, representing samples from different radial strips, were used for the validation set. Mean tracheid length for the calibration set was 2.26 mm with standard deviation of 0.65 mm, while the validation set had a mean of 2.28 mm and standard deviation of 0.63 mm. The range in tracheid length for the calibration (1.06–4.00 mm) and validation (1.06–3.82 mm) sets is similar. Tracheid width had a mean of 40.3 µm and standard deviation of 2.9 µm for the calibration set, and mean of 41.1 µm and standard deviation of 2.6 µm for the validation set. Calibration and validation datasets had similar summary statistics for both properties, indicating that the duplex sample selection algorithm (Snee 1977) successfully selected calibration and validation samples with similar tracheid property variation using the variation present in the NIR spectra. The ranges for tracheid width were also similar between the calibration (31.9–48.9 µm) and validation (33.4–47.6 µm) sets.

Table 2 Summary statistics of tracheid length (mm) and tracheid width (µm) for the calibration and validation sets

Property	Calibration set					Validation set				
	N	Mean	Min	Max	SD	*N*	Mean	Min	Max	SD
Tracheid length (mm)	1020	2.26	1.06	4.00	0.65	998	2.28	1.06	3.82	0.63
Tracheid width (µm)		40.3	31.9	48.9	2.9		41.06	33.4	47.6	2.6

The calibration models for tracheid length and width were carried out using the raw spectra (no spectral preprocessing) and their second derivatives (Savitzky–Golay approach); the summary statistics are listed in Table 3. The second-derivative data performed only slightly better than the untreated spectra for both tracheid properties. While the second-derivative spectral data did not significantly improve the performance of the calibration models, it did result in a reduction in the number of factors in the tracheid length model to 7, and 7 for the tracheid width model, both down from 10 with raw spectra for tracheid length and 9 for tracheid width.

For tracheid length, using a seven-factor model with the second-derivative spectra had $R^2 = 0.90$ and SECV = 0.21 mm. The calibration model, when applied to the validation set, had similar summary statistics with $R_p^2 = 0.87$ and SEP = 0.23 mm. The tracheid length RPD values for the calibration and validation sets were 3.1 (RPD_{cv}) and 2.8 (RPD_p), respectively. As these RPDs are between the thresholds necessary for screening (RPD ≥ 2.5) and quality control (RPD ≥ 5), the models are at least appropriate for screening in breeding programs (AACC 1999). It is important to note that the AACC standard was created for cereal grains and not wood, and these threshold values are important for predictions when the properties of a single sample are of interest. However, the vast majority of NIR prediction models developed for wood properties is to measure population statistics using multiple samples, and thus, differences between the RPD thresholds are less important as the number of measurements increases. The relationship between measured values and NIR-predicted values for tracheid length is shown in Fig. 2.

The tracheid length SEP in the current study of 0.23 mm was similar to that reported by Schimleck et al. (2004a) ($R_p^2 = 0.86$, SEP = 0.25 mm). The current study evaluated a considerably larger number of samples (2018 samples vs. 40 samples) and thus included more variation in site, climate, genetics, and soil type. The study results are very similar also with respect that differences may arise due to the type of optical fiber analyzer used; Schimleck et al. (2004a) used a Kajaani fiber quality analyzer, while here a TechPap MorFi instrument was used. However, while differences between optical analyzers have been reported, the instruments themselves tend to be very repeatable, and thus, differences between analyzers are consistent (Guay et al. 2005; Li et al. 2011). The calibration model statistics reported here are stronger than those reported by Hauksson et al. (2001) from NIR samples collected

Table 3 Near-infrared spectroscopy results for tracheid length (mm) and tracheid width (µm) for the calibration and validation sets

Property	Preprocessing	Calibration set					Validation set		
		No. of factors	R^2	SECV	RMSECV	RPDcv	R_p^2	SEP	RPDp
Tracheid length (mm)	None	10	0.87	0.23	0.25	2.8	0.85	0.25	2.6
	2ndDer	7	0.90	0.21	0.23	3.1	0.87	0.23	2.8
Tracheid width (µm)	None	9	0.61	1.8	1.7	1.6	0.55	1.8	1.5
	2ndDer	7	0.66	1.7	1.7	1.7	0.61	1.6	1.6

2ndDer = second derivative calculated from Savitzky–Golay data pretreatment

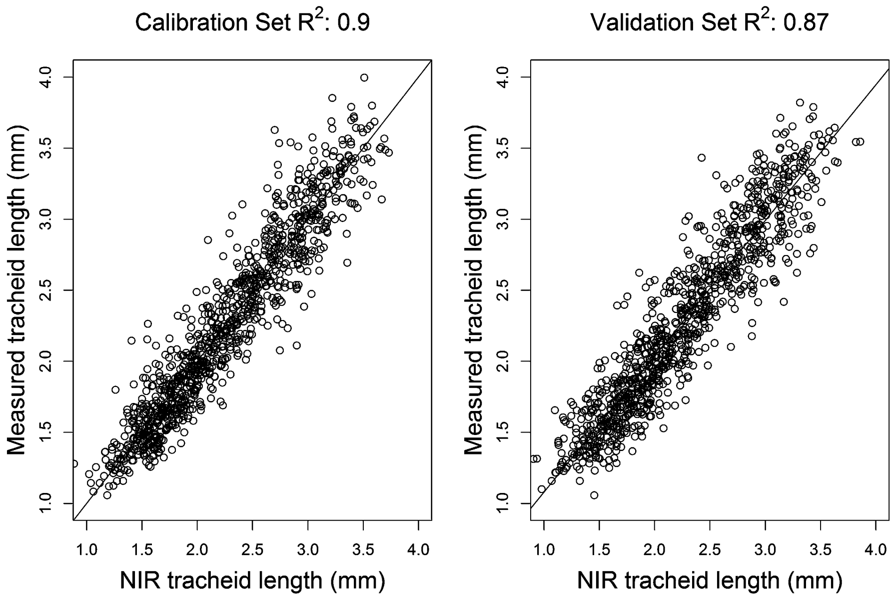

Fig. 2 Calibration and validation set plots of tracheid length versus the near-infrared spectroscopy fitted values predicted from a model developed on the calibration set

from milled wood of Norway spruce (*Picea abies*) ($R_p^2 = 0.52$). Using longleaf pine ($N = 300$), Via et al. (2005b) showed weaker calibration model statistics ($R_p^2 = 0.72$) for tracheid length than reported here; they used a different NIR instrument (Thermo Nicolet Instruments Nexus 670 Fourier transform); however, the specifications are similar to the FOSS that was used here (wavelength range from 1000 nm to 2500 with 1-nm interval). The differences observed between the two studies may be due to the lack of humidity control in the scanning room used by Via et al. (2005b), or related to the area scanned. Via et al. (2005b) scanned the latewood area of the wood next to the wood that was macerated, but here the wood was scanned and macerated in the same area.

Sykes et al. (2005) used the transmittance NIR technique instead of diffuse reflectance NIR technique used here to predict tracheid length for loblolly pine. They transmitted light through 200-μm microtomed sections collected from two sites. The data from tracheid length were reported in an earlier study; however, discussion on the measurement of length was not discussed (Sykes et al. 2003). The samples from one site were used to develop calibration models and then used to predict the second-site characteristics. Overall, they found moderate results ($R_p^2 = 0.43$, SEP = 0.49 mm). These results suggest that diffuse reflectance NIR spectroscopy has significant advantages over transmittance NIR spectroscopy because microtomed sections are time-consuming to prepare and the models performance was worse than those found in studies using diffuse reflectance NIR. However, the use of single-site models may have presented problems with the prediction accuracy because of the lack of variation found in the calibration dataset (Jones et al. 2005a).

For tracheid width, using a seven-factor model with the second-derivative spectra had $R^2 = 0.66$ with SECV = 1.7 µm. When the model was used to predict tracheid width for the validation dataset, similar statistics were obtained ($R_p^2 = 0.61$ and SEP = 1.6 µm). The tracheid width RPD values for calibration and validation sets were 1.7 and 1.6 (RPD_{cv} and RPD_p). One important factor to consider herein is the operational specifications of the instrumentation used to measure the tracheids. Specifically, the camera resolution for the MorFi Compact Fiber and Shive Analyzer system is 4 µm, and thus, the NIR model performance was within the measurement error (± 2 µm) for the system. The relationship between measured values and NIR-predicted values for tracheid width is shown in Fig. 3. The model shows some nonlinear behavior, particularly at low tracheid widths which may be the result of a combination of factors. Via and Jiang (2013) discuss the nonlinear behavior observed between light absorbance and wood density, and they found nonlinear behavior of bending strength and stiffness with NIR predictions. For tracheid width, differences in the chemistries between earlywood and latewood zones, when combined with differences in the light absorbance of low-porosity latewood and higher-porosity earlywood, may be causing the slightly nonlinear behavior in the models. Another possible reason for the slightly nonlinear behavior could be related to measurement errors resulting from the camera accuracy (± 2 µm). Some research has used nonlinear modeling techniques to improve the predictions; for example, Mora and Schimleck (2010) demonstrated the effectiveness of using kernel regression methods to improve nonlinearity in NIR data.

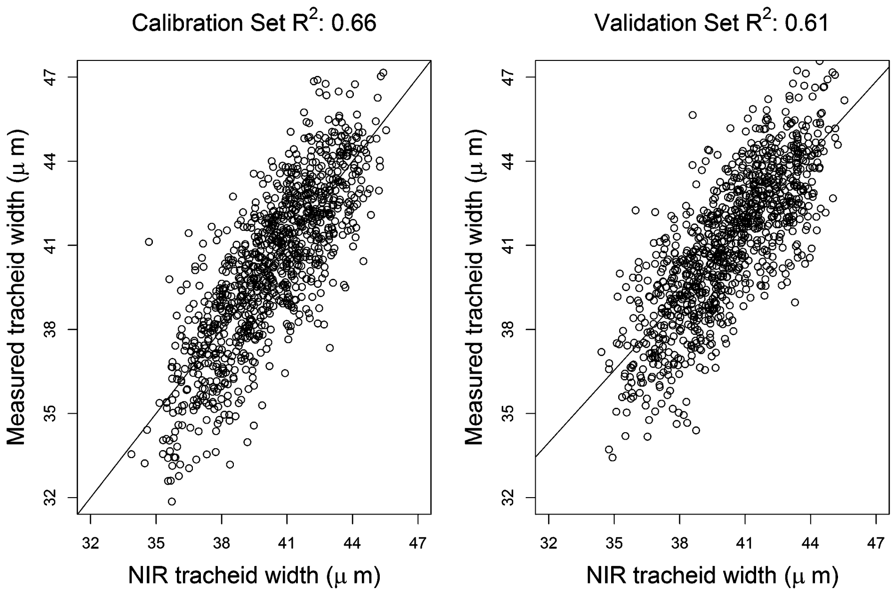

Fig. 3 Calibration and validation set plots of tracheid width versus the near-infrared spectroscopy fitted values predicted from a model developed on the calibration set

The SEP for tracheid width (1.6 μm) was similar to the results reported by Schimleck and Evans (2004) for radiata pine (*Pinus radiata*) for radial diameter (SEP = 1.9 μm) and tangential diameter (SEP = 1.7 μm) obtained using the SilviScan system. In a study on loblolly pine using the SilviScan system, Jones et al. (2005a) found lower R_p^2 values for radial (0.29) and tangential diameter (0.59), but similar SEP values for radial (1.8 μm) and tangential (1.1 μm) diameters. Compared to tracheid length with a range of values from 1.06 to 4.00 mm, tracheid width has a range of values from 31.9 to 48.9 μm and thus shows less radial variation from pith to bark (Evans 1994); this low variability may be one reason why tracheid width predictions are less accurate than tracheid length predictions. However, because the tracheid width SEP is within the measurement error of the camera (± 2-μm), it is difficult to say with certainty what the limiting factor is with regard to the calibration model. The measurement error for the MorFi has greater precision than most other optical fiber analyzers except those instruments that have a two-camera setup where one camera measures length, and the second measures width (Guay et al. 2005). It is also possible that stronger calibration and validation statistics were acquired for tracheid length because of the orientation of the NIR beam to the sample compared to tracheid width (Evans 1994; Schimleck and Evans 2004; Jones et al. 2005a).

Studies utilizing reference data provided by the SilviScan system have found stronger calibration models for coarseness, a measure of mass per unit length (μg/m), and cell wall thickness than for radial and tangential diameters. For example in radiata pine, Schimleck and Evans (2004) reported R_p^2 = 0.91, and SEP = 76.6 μg/m for coarseness, and R_p^2 = 0.88, SEP = 0.5 μm for wall thickness. Jones et al. (2005a) reported similar relationships for loblolly pine (coarseness R_p^2 = 0.82, SEP = 45.1 μg/m and wall thickness R_p^2 = 0.86, SEP = 0.3 μm). Overall, it appears that the density-related pulp properties have better NIR relationships than the width properties. The fact that tangential width shows little variation from pith to bark (Schimleck et al. 2004b) may be another cause of the lack of good fit statistics.

Separate calibration models were then developed for length and width from data specific to one region, and then the models used to predict the tracheid properties of samples from the other regions. For tracheid length, using the region 1 samples to develop the calibration model, the results of predicting the other regions were R_p^2 = 0.87, SEP = 0.23 mm. Similar results were obtained for region 2 (R_p^2 = 0.85, SEP = 0.25 mm), region 3 (R_p^2 = 0.85, SEP = 0.26 mm), region 4 (R_p^2 = 0.86, SEP = 0.25 mm), region 5 (R_p^2 = 0.87, SEP = 0.23 mm), and region 6 (R_p^2 = 0.89, SEP = 0.23 mm); all models used seven factors. For tracheid width, using the region 1 samples to develop the calibration model, the results of predicting the other regions were R_p^2 = 0.56, SEP = 1.8 μm. Similar results were obtained for region 2 (R_p^2 = 0.51, SEP = 2.0 μm), region 3 (R_p^2 = 0.58, SEP = 2.0 μm), region 4 (R_p^2 = 0.44, SEP = 2.2 μm), region 5 (R_p^2 = 0.55, SEP = 1.8 μm), and region 6 (R_p^2 = 0.61, SEP = 2.1 μm); all models used seven factors. For tracheid length, the region-specific models performed similarly to the overall calibration model, whereas the tracheid width models had slightly lower accuracy, particularly from region 2 (N = 105), region 3 (N = 166), and region 4 (N = 129), which had the least number of samples macerated compared to region 1, 5, and 6. Jones et al. (2005a) demonstrated that the prediction accuracy of tracheid properties for new sites can be

Table 4 Wavelengths of importance found through local maxima values from the coefficient of determination values by regressing tracheid length against each near-infrared spectra wavelength

Wavelength	Tracheid length (mm)		Structural component
	R^2	RMSE	
1160	0.46	0.47	Cellulose
1226	0.65	0.38	Cellulose
1416	0.57	0.42	Lignin
1486	0.46	0.47	Cellulose
1516	0.38	0.50	Cellulose
1542	0.77	0.31	Cellulose
1600	0.55	0.43	Cellulose
1780	0.54	0.44	Cellulose
1832	0.44	0.48	Cellulose
2082	0.41	0.49	Cellulose
2324	0.34	0.52	Hemicellulose

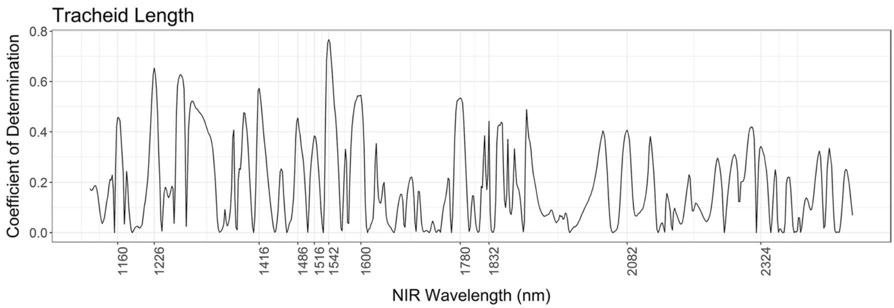

Fig. 4 Near-infrared spectroscopy wavelengths of importance with tracheid length. The wavelengths are attributed to cellulose (bands: 1160, 1226, 1486, 1516, 1542, 1600, 1780, 1832, 2082), hemicellulose (band: 2324), and lignin (band: 1416)

improved considerably when the addition of one sample from a new site is added to the calibration model. This finding is one of several studies that have concluded that calibration model accuracy improves when new sites are included in the calibration set because the subtle amount of variation from new samples can be accounted for in the model (Guthrie et al. 2005; Jones et al. 2005b; Dahlen et al. 2017). The results found here suggest that model accuracy can still be maintained when predicting samples from new sites provided the calibration model contains a large enough sample size to account for the resource variation. The slightly nonlinear trend for tracheid width was also observed with the region-specific models.

Wavelengths of importance were explored for tracheid length and not tracheid width, because of the strength of the models developed for tracheid length. Tracheid length was regressed against each of the second-derivative NIR wavelengths response. The models afforded a plot with the individual wavelengths plotted along the *x*-axis and coefficient of determination for the linear model along the *y*-axis. In doing so, the NIR bands assigned to cellulose, hemicellulose, or lignin by Schwanninger et al. (2011) imparting the greatest effect on the models could be determined by finding the local maxima (Table 4, Fig. 4). Several bands that can be attributed to cellulose bond vibrations include those at 1160, 1486, 1516, 1542, 1600, 1780, 1832, and 2082 nm. A hemicellulose band (2324 nm) and a lignin band (1416 nm) were also identified in the plot. The two best wavelengths were attributed to cellulose (1542 nm, $R^2 = 0.77$, RMSE = 0.31 mm; 1226 nm, $R^2 = 0.65$, RMSE = 0.38 mm) (Schwanninger et al. 2011). The third best relationship for predicting tracheid length was the 1416 nm lignin band ($R^2 = 0.57$, RMSE = 0.42 mm). Tracheid length increases from pith to bark (Via et al. 2005b; Mäkinen et al. 2007), as does cellulose content while lignin decreases (Uprichard and Lloyd 1980). Given the strong relationship observed here between wavelengths attributed to cellulose, the changes appear to be related. The caveat herein with band assignments is that with the second derivative, bands can shift as much as 5 nm because of the effect of data smoothing which is necessary for calculating the derivative (Schwanninger et al. 2011). Thus, band assignments in the literature may differ slightly if found using the untreated raw spectra or after data pretreatments. Re-running the analysis separately using samples from each of the six regions did not change the wavelengths of importance. A multiple linear regression model for tracheid length using stepwise regression was constructed with the final bands selected being at 1160, 1226, 1416, 1486, 1542, and 2082 nm. Other combinations of bands had some wavelengths with variance inflation factors over 10, which indicates collinearity among the selected parameters. The adjusted R^2 for the multiple regression model was 0.81 and the RMSE was 0.28 mm, which nearly equaled the performance of the PLS model. Given the strong relationship between certain wavelengths and tracheid length, there exists the possibility that a NIR instrument could be built to measure selected wavelengths. This would result in a simpler, more affordable system that potentially would be attractive to companies seeking a lower cost method for tracheid analysis.

The application of NIR spectroscopy to go beyond feasibility studies conducted on a small number of samples in the laboratory has increasingly been demonstrated in recent years (Leblon et al. 2013). Downes et al. (2010) successfully developed and applied calibration models of cellulose content, Kraft pulp yield and density in eucalypt from over 1000 samples using a Bruker MPA instrument. Meder et al. (2011b) utilized a fiber-optic-equipped NIR system with a linear drive to predict wood properties in 1-mm radial resolution from pith to bark for eucalypt and radiata pine. The use of hyperspectral imaging systems has increasingly been used to predict and visualize the spatial patterns for wood chemistry (Thumm et al. 2010), compression wood (Meder and Meglen 2012), MFA and density on small samples (Ma et al. 2017), and moisture content and density of lumber (Haddadi et al. 2015a, b). In addition to measurements on core, disk, or lumber samples, the use of portable instruments to predict measurements on standing trees has been demonstrated. Meder et al. (2011a) compared a handheld NIR (Polychromix Phazir) to a laboratory instrument (Bruker MPA) and found excellent correlations ($R > 0.90$) for both cellulose and Kraft pulp yield in eucalypt. These developments are promising for the utilization of NIR spectroscopy to make decisions in the forest industry (Meder et al. 2010; Meder and Schimleck 2011).

Unfortunately, there are still significant limitations for collecting NIR reference tracheid length data because of the maceration process. When disk samples are available, the measurement is straightforward; however, this requires tree felling and in recent years more information on wood properties can be extracted from increment cores which allow for more rapid measurements to be conducted, especially when they are paired with the SilviScan system (Evans 1994). When measuring tracheid length from increment cores, the effect that cut ends have on the measurements is of great concern because as core size decreases the amount of cut tracheids increases which negatively affects the accuracy of the measurement (Bergqvist et al. 1997). Thus, in order to minimize the effect of cut tracheids, increment cores should be avoided for sampling tracheid length unless the sides of the core are cut off; however, this technique still does not work well with cores less than 12 mm in diameter. Regardless of whether using disk or core samples, the effect of cut tracheids is still observed in any sample macerated and thus the reliance on weighted length measurements instead of arithmetic measurements when using optical fiber analyzers. Mörling et al. (2003) developed a method to predict the true length based on the calculated distribution of the fines and the tracheids. They found little variation in the distribution of fines, and thus, they were able to utilize this information to calculate the distribution of the tracheids and find the true mean length. Recently, Chen et al. (2016a) refined this technique by using the expectation–maximization method and compared the calculated results to weighted length obtained from the optical analyzer to the mean length as measured on un-cut tracheids using a microscope. They found that the expectation–maximization method prediction of mean length was more accurate than using weighted length, and they employed the technique in a progeny test to evaluate the tracheid length and other wood and fiber properties from 524 families (Chen et al. 2016b). The method appears to have promise for potentially more accurate predictions of tracheid length and when combined with NIR spectroscopy would help yield rapid and accurate predictions.

Conclusion

The purpose of this study was to develop NIR spectral models to predict the tracheid properties of loblolly pine collected from across the Southeast. The models were developed by scanning 1842 samples from pith to bark at 10-mm radial resolution using NIR spectroscopy and measuring the tracheid properties using an optical instrument. The prediction statistics determined here demonstrate that NIR models developed and applied to samples collected from data across the region can be accurate at predicting for tracheid length (SEP = 0.23 mm). The tracheid width relationships were not as strong as the length models but within the measurement error of the camera (SEP = 1.6 µm, camera ± 2 µm). Wavelength 1542, attributed to cellulose, had the strongest linear relationship with tracheid length (R^2 = 0.77, RMSE = 0.31 mm). The study shows that robust region-wide NIR calibration models can be successfully developed for predicting the tracheid properties of loblolly pine.

Acknowledgements This research was possible through support from NIFA McIntire-Stennis Project 1006098 and the Wood Quality Consortium (WQC) at the University of Georgia. The authors wish to thank NIFA and the WQC for funding this project.

References

AACC (1999) AACC method 39-00.01. Near-infrared methods—guidelines for model development and maintenance. AACC, St. Paul

Antony F, Schimleck LR, Daniels RF, Clark A III, Hall DB (2010) Modeling the longitudinal variation in wood specific gravity of planted loblolly pine (*Pinus taeda*) in the United States. Can J For Res 40(12):2439–2451

Bergqvist G, Bergsten U, Ahlqvist B (1997) Effect of radial increment core diameter on tracheid length measurement in Norway spruce. Wood Sci Technol 31:241–250

Borders BE, Bailey RL (2001) Loblolly pine—pushing the limits of growth. South J Appl For 25(2):69–74

Carvalho MG, Ferreira PJ, Martins AA, Figueiredo MM (1997) A comparative study of two automated techniques for measuring fiber length. Tappi J 80(2):137–142

Chen ZQ, Abramowicz K, Raczkowski R, Ganea S, Wu HX, Lundqvist SO, Mörling T, Sjöstedt de Luna S, Rosario M, Gil MRG, Mellerowicz EJ (2016a) Method for accurate fiber length determination from increment cores for large-scale population analyses in Norway spruce. Holzforschung 70(9):829–838

Chen ZQ, Karlsson B, Mörling T, Olsson L, Mellerowicz EJ, Wu HX, Lundqvist SO, Gil MRG (2016b) Genetic analysis of fiber dimensions and their correlation with stem diameter and solid-wood properties in Norway spruce. Tree Genet Genomes 12:123

Dahlen J, Diaz I, Schimleck L, Jones PD (2017) Near-infrared spectroscopy prediction of southern pine No. 2 lumber physical and mechanical properties. Wood Sci Technol 51(2):309–322

Downes G, Meder R, Harwood C (2010) A multi-site, multi-species near infrared calibration for the prediction of cellulose content in eucalypt woodmeal. J Near Infrared Spectrosc 18:381–387

Evans R (1994) Rapid measurement of the transverse dimensions of tracheids in radial wood sections from *Pinus radiata*. Holzforschung 48(2):168–172

Fox TR, Jokela EJ, Allen HL (2007) The development of pine plantation silviculture in the southern United States. J For 105(7):337–347

Franklin G (1945) Preparation of thin sections of synthetic resins and wood-resin composites, and a new macerating method for wood. Nature 155(3924):51–55

Gindl W, Teischinger A, Schwanninger M, Hinterstoisser B (2001) The relationship between near infrared spectra of radial wood surfaces and wood mechanical properties. J Near Infrared Spectrosc 9:255–261

Granato D, Ares G (2013) Mathematical and statistical methods in food science and technology. Wiley, New York

Guay D, Sutherland NR, Rantanen W, Malandri N, Stephens A, Mattingly K, Schneider M (2005) Comparison of fiber length analyzers. In: TAPPI practical papermaking conference proceedings, 22–26 May 2005

Guthrie JA, Reid DJ, Walsh KB (2005) Assessment of internal quality attributes of mandarin fruit. 2. NIR calibration robustness. Aust J Agric Res 56:417–426

Haartveit EY, Flæte PO (2006) Rapid prediction of basic wood properties by near infrared spectroscopy. N Z J For Sci 36(2/3):393–407

Haddadi A, Burger J, Leblon B, Pirouz Z, Groves K, Nader J (2015a) Using near-infrared hyperspectral images on subalpine fire board. Part 1: moisture content estimation. Wood Mater Sci Eng 10(1):27–40

Haddadi A, Burger J, Leblon B, Pirouz Z, Groves K, Nader J (2015b) Using near-infrared hyperspectral images on subalpine fire board. Part 2: density and basic specific gravity estimation. Wood Mater Sci Eng 10(1):41–56

Hauksson JB, Bergqvist G, Bergsten U, Sjöström M, Edlund U (2001) Prediction of basic wood properties for Norway spruce. Interpretation of near infrared spectroscopy data using partial least squares regression. Wood Sci Technol 35(6):475–485

Hein PRG, Brancheriau L, Trugilho PF, Lima JT, Chaix G (2010) Resonance and near infrared spectroscopy for evaluating dynamic wood properties. J Near Infrared Spectrosc 18(6):443–454

Hirn U, Bauer W (2006) A review of image analysis based methods to evaluate fiber properties. Lenzing Berichte 86:96–105

Hodge G, Woodbridge W (2004) Use of near infrared spectroscopy to predict lignin content in tropical and sub-tropical pines. J Near Infrared Spectrosc 12(6):381–390

Inagaki T, Schwanninger M, Kato R, Kurata Y, Thanapase W, Puthson P, Tsuchikawa S (2012) *Eucalyptus camaldulensis* density and fiber length estimated by near-infrared spectroscopy. Wood Sci Technol 46(1–3):143–155

Jones PD, Schimleck LR, Peter GF, Daniels RF, Clark A III (2005a) Non-destructive estimation of *Pinus taeda* L tracheid morphological characteristics for samples from a wide range of sites in Georgia. Wood Sci Technol 39(7):529–545

Jones PD, Schimleck LR, Peter GF, Daniels RF, Clark A III (2005b) Non-destructive estimation of *Pinus taeda* L. wood properties from a wide range of sites in Georgia. Can J For Res 35:85–92

Jones PD, Schimleck LR, Peter GF, Daniels RF, Clark A III (2006) Nondestructive estimation of wood chemical composition of sections of radial wood strips by diffuse reflectance near infrared spectroscopy. Wood Sci Technol 40(8):709–720

Jones PD, Schimleck LR, So CL, Clark A III, Daniels RF (2007) High resolution scanning of radial strips cut from increment cores by near infrared spectroscopy. IAWA J 28(4):473–484

Jordan L, He R, Hall DB, Clark A III, Daniels RF (2007) Variation in loblolly pine ring microfibril angle in the Southeastern United States. Wood Fiber Sci 39(2):352–363

Jordan L, Clark A, Schimleck LR, Hall DB, Daniels RF (2008) Regional variation in wood specific gravity of planted loblolly pine in the United States. Can J For Res 38(4):698–710

Kahle D, Wickham H (2013) ggmap: spatial visualization with ggplot2. R J 5(1):144–161

Kelley SS, Rials TG, Groom LR, So CL (2004) Use of near infrared spectroscopy to predict the mechanical properties of six softwoods. Holzforschung 58(3):252–260

Kennard RW, Stone LA (1969) Computer aided design of experiments. Technometrics 11(1):137–148

Ladell JT (1959) A new method of measuring tracheid length. Forestry 32:124–125

Leblon B, Adepipe O, Hans G, Haddadi A, Tsuchikawa S, Burger J, Stirling R, Pirouz Z, Groves K, Nader J, LaRocpue A (2013) A review of near-infrared spectroscopy for monitoring moisture content and density of solid wood. For Chron 89(5):595–606

Li B, Bandekar R, Zha Q, Alsaggaf A, Ni Y (2011) Fiber quality analysis: OpTest fiber quality analyzer versus L&W fiber tester. Ind Eng Chem Res 50(22):12572–12578

Ma T, Inagaki T, Tsuchikawa S (2017) Calibration of SilviScan data of *Cryptomeria japonica* wood concerning density and microfibril angles with NIR hyperspectral imaging with high spatial resolution. Holzforschung 71(4):341–347

Mäkinen H, Jaakkola T, Piispanen R, Saranpää P (2007) Predicting wood and tracheid properties of Norway spruce. For Ecol Manage 241:175–188

McKeand S, Mullin T, Bryam T, White T (2003) Deployment of genetically improved loblolly and slash pines in the south. J For 101(3):32–37

McKenzie AW (1994) A guide to pulp evaluation. CSIRO, Melbourne

Meder R, Meglen RR (2012) Near infrared spectroscopic and hyperspectral imaging of compression wood in *Pinus radiata* D. Don. J Near Infrared Spectrosc 20:583–589

Meder R, Schimleck L (2011) Has the time finally come for NIR in the forestry sector? J Near Infrared Spectrosc 19(5):5

Meder R, Trung T, Schimleck L (2010) Seeing the wood in the trees: unleashing the secrets of wood via near infrared spectroscopy. J Near Infrared Spectrosc 18:5–7

Meder R, Brawner JT, Downes GM, Ebdon N (2011a) Towards the in-forest assessment of Kraft pulp yield: comparing the performance of laboratory and hand-held instruments and their value in screening breeding trials. J Near Infrared Spectrosc 19:421–429

Meder R, Marston D, Ebdon N, Evans R (2011b) Spatially-resolved radial scanning of tree increment cores for near infrared prediction of microfibril angle and chemical composition. J Near Infrared Spectrosc 18:499–505

Mevik B-H, Wehrens R, Hovde Liland K (2013) pls: partial least squares and principal component regression. R package version 2.4-3. http://CRAN.R-project.org/package=pls

Moore JR, Cown DJ (2017) Corewood (juvenile wood) and its impact on wood utilisation. Curr For Rep 3:107–118

Mora C, Schimleck LR (2008) On the selection of samples for multivariate regression analysis: application to near infrared (NIR) calibration models. Can J For Res 38(10):2626–2634

Mora C, Schimleck LR (2010) Kernel regression methods for the prediction of wood properties of *Pinus taeda* using near infrared spectroscopy. Wood Sci Technol 44:561–578

Mörling T, Sjöstedt-de Luna S, Svensson I, Fries A, Ericsson T (2003) A method to estimate fibre length distribution in conifers based on wood samples from increment cores. Holzforschung 57(3):248–254

Niskanen K (1998) Paper physics. TAPPI Press, Vancouver

Paavilainen L (1993) Importance of cross-dimensional fibre properties and coarseness for the characterisation of softwood sulphate pulp. Pap Puu 75(5):343–351

Pereira H, Santos AJA, Anjos O (2015) Fibre morphological characteristics of kraft pulps of *Acacia melanoxylon* estimated by NIR-PLS-R models. Materials 9(1):8

Pulkkinen I, Ala-Kaila K, Aittamaa J (2006) Characterization of wood fibers using fiber property distributions. Chem Eng Process 45(7):546–554

Raymond CA, Schimleck LR (2002) Development of near infrared reflectance analysis calibrations for estimating genetic parameters for cellulose content in *Eucalyptus globulus*. Can J For Res 32(1):170–176

R Core Team (2017) R: a language and environment for statistical computing. R Foundation for Statistical Computing, Vienna. http://www.R-project.org/

RStudio (2017) RStudio: integrated development environment for R. Boston, MA. https://www.rstudio.com/

Savitzky A, Golay MJE (1964) Smoothing and differentiation of data by simplified least squares procedures. Anal Chem 1964(36):1627–1639

Schimleck LR, Evans R (2004) Estimation of *Pinus radiata* D. tracheid morphological characteristics by near infrared spectroscopy. Holzforschung 58(1):66–73

Schimleck LR, French J (2002) Application of NIR spectroscopy to clonal *Eucalyptus globulus* samples covering a narrow range of pulp yield. Appita J 55(2):149–154

Schimleck LR, Mora C, Daniels RF (2003) Estimation of the physical wood properties of green *Pinus taeda* radial samples by near infrared spectroscopy. Can J For Res 33(12):2297–2305

Schimleck LR, Jones PD, Peter GF, Daniels RF, Clark A III (2004a) Nondestructive estimation of tracheid length from sections of radial wood strips by near infrared spectroscopy. Holzforschung 58:375–381

Schimleck LR, Mora C, Daniels RF (2004b) Estimation of tracheid morphological characteristics of green *Pinus taeda* L. radial strips by near infrared spectroscopy. Wood Fiber Sci 36(4):527–535

Schimleck LR, Jones PD, Clark A III, Daniels RF, Peter GF (2005) Near infrared spectroscopy for the nondestructive estimation of clear wood properties of *Pinus taeda* L. from the southern United States. For Prod J 55(12):21–28

Schimleck LR, Kube PD, Raymond CA, Michell AJ, French J (2006) Extending near infrared reflectance (NIR) pulp yield calibrations to new sites and species. J Wood Chem Technol 26(4):299–311

Schimleck LR, Hodge GR, Woodbridge W (2010) Toward global calibrations for estimating the wood properties of tropical, sub-tropical and temperate pine species. J Near Infrared Spectrosc 18:355–365

Schultz RP (1997) Loblolly pine: the ecology and culture of loblolly pine (*Pinus taeda* L.). US Department of Agriculture, Forest Service, Washington

Schwanninger M, Rodrigues JC, Fackler K (2011) A review of band assignments in near infrared spectra of wood and wood components. J Near Infrared Spectrosc 19:287–308

Signal Developers (2013) Signal: signal processing. http://r-forge.r-project.org/projects/signal/

Smook GA (2016) Handbook for pulp & paper technologists. TAPPI Press, Vancouver

Snee RD (1977) Validation of regression models: methods and examples. Technometrics 19(4):415–428

So CL, Via BK, Groom LH, Schimleck LR, Shupe TF, Kelley SS, Rials TG (2004) Near infrared spectroscopy in the forest products industry. For Prod J 54(3):7–16

Stevens A, Ramirez-Lopez L (2013) An introduction to the prospectr package. R package Vignette R package version 0.1.3

Sykes RW, Isik F, Li B, Kadla J, H-m Chang (2003) Genetic variation of juvenile wood properties in a loblolly pine progeny test. Tappi J 2(12):3–8

Sykes RW, Li B, Hodge G, Goldfarb B, Kadla J, H-m Chang (2005) Prediction of loblolly pine wood properties using transmittance near-infrared spectroscopy. Can J For Res 35:2423–2431

Thumm A, Riddell M, Nanayakkara B, Harrington J, Meder R (2010) Near infrared hyperspectral imaging applied to mapping chemical composition in wood samples. J Near Infrared Spectrosc 18:507–515

Tsuchikawa S (2007) A review of recent near infrared research for wood and paper. Appl Spectrosc Rev 42(1):43–71

Tsuchikawa S, Kobori H (2015) A review of recent application of near infrared spectroscopy to wood science and technology. J Wood Sci 61:213–220

Tsuchikawa S, Schwanninger M (2013) A review of recent near infrared research for wood and paper (part 2). Appl Spectrosc Rev 48(7):560–587

Uprichard JM, Lloyd JA (1980) Influence of tree age on the chemical composition of radiata pine. N Z J For Sci 10(3):551–557

Vahey DW, Zhu JY, Scott CT (2007) Wood density and anatomical properties in suppressed-growth trees: comparison of two methods. Wood Fiber Sci 39(3):462–471

Varmuza K, Filzmoser P (2009) Introduction to multivariate statistical analysis in chemometrics. CRC Press, Boca Raton

Via BK, Jiang W (2013) Nonlinear multivariate modeling of strand mechanical properties with near-infrared spectroscopy. For Chron 89(5):621–630

Via BK, Stine M, Shupe TF, So CL, Groom L (2004) Genetic improvement of fiber length and coarseness based on paper product performance and material variability—a review. IAWA J 25(4):401–414

Via BK, So CL, Shupe TF, Eckhardt LG, Stine M, Groom L (2005a) Prediction of wood mechanical and chemical properties in the presence and absence of blue stain using two near infrared instruments. J Near Infrared Spectrosc 13(4):201–212

Via BK, Shupe TF, Stine M, So CL, Groom LH (2005b) Tracheid length prediction in *Pinus palustris* by means of near infrared spectroscopy: the influence of age. Holz Roh- Werkst 63(3):231–236

Wang T, Aitken SN (2001) Variation in xylem anatomy of selected populations of lodgepole pine. Can J For Res 31(11):2049–2057

Wear DN, Greis JG (2002) Southern forest resource assessment: summary of findings. J For 100(7):6–14

White DE, Courchene C, McDonough T, Schimleck L, Jones D, Purnell R, Goyal G (2009) Effects of specific gravity and wood chemical content on the pulp yield of loblolly pine. Tappi J 92(4):29–34

Wickham H (2009) ggplot2: elegant graphics for data analysis. Springer, New York

Wickham H, Francois R (2016) dplyr: a grammar of data manipulation. R package version 0.4.3. https://CRAN.R-project.org/package=dplyr

Wilkins AP, Bamber RK (1983) A comparison between Ladell's wood section method and the macerated wood method for tracheid length determination. IAWA Bull 4(4):245–247

Williams PC, Sobering D (1993) Comparison of commercial near infrared transmittance and reflectance instruments for analysis of whole grains and seeds. J Near Infrared Spectrosc 1(1):25–32

Yeh TF, Hm Chang, Kadla JF (2004) Rapid prediction of solid wood lignin content using transmittance near-infrared spectroscopy. J Agric Food Chem 52(6):1435–1439

Zhao D, Kane M, Borders BE (2011) Growth responses to planting density and management intensity in loblolly pine plantations in the southeastern USA Lower Coastal Plain. Ann For Sci 68(3):625–635

Zhao D, Kane MB, Teskey RO, Fox TR, Albaugh TJ, Allen HL, Rubilar RA (2016) Maximum response of loblolly pine plantations to silvicultural management in the southern United States. For Ecol Manag 375:105–111

Zobel BJ, Van Buijtenen JP (1989) Wood variation: its causes and control. Springer, Berlin